Connectivity Preservation and Collision Avoidance Control for Spacecraft Formation Flying with Bounded Actuation

Xianghong Xue, Xiaokui Yue, and Jianping Yuan

Abstract This paper considers connectivity preservation and collision avoidance controller design for spacecraft formation flying with bounded actuation. A distributed controller with bounded artificial potential function and indirect couplings is proposed. It is assumed that all spacecraft can only obtain the states of their neighbors. The communication graph between the spacecraft is modeled via distance-induced proximity graph. A bounded potential function is presented to tackle connectivity preservation and collision avoidance problems. The spacecraft-proxy couplings address the actuator saturation constraints by designing a virtual proxy for each spacecraft. The inter-proxy artificial potential function fulfills the coordination of all spacecraft. Numerical simulations confirm the effectiveness of the anti-saturation distributed connectivity preservation controller.

Keywords Spacecraft formation flying · Bounded actuation · Artificial potential function · Connectivity preservation

1 Introduction

Spacecraft formation flying (SFF) has gained considerable intentions due to its flexibility and robustness [1]. One of the critical issues for SFF is to design distributed controllers to achieve formation maintenance or reconfiguration. The fulfillments of distributed controllers require the connectivity of the communication graphs at all

X. Xue (✉) · X. Yue · J. Yuan
National Key Laboratory of Aerospace Flight Dynamics, Northwestern Polytechnical University, Xi'an, People's Republic of China
e-mail: xhxue@mail.nwpu.edu.cn

X. Yue
e-mail: xkyue@nwpu.edu.cn

J. Yuan
e-mail: jyuan@nwpu.edu.cn

L. Yan et al. (eds.), *Advances in Guidance, Navigation and Control*, Lecture Notes in Electrical Engineering 644,
https://doi.org/10.1007/978-981-15-8155-7_307

time [2, 3]. However, constrained by the communication range of the spacecraft, the graph's connectivity might be destroyed by the movements of the spacecraft. A more practical question is how to maintain the connectivity of the graph [4].

The connectivity preservation controllers have been studied in multi-agent systems and mobile robotic systems in the last decade [5, 6]. The connectivity preservation methods mainly include the optimization-based methods [7, 8] and the artificial potential function (APF) based methods [9, 10]. The optimization-based method fulfills connectivity preservation by maximizing algebraic connectivity of the graph in [7]. Ji and Egerstedt proposed a distributed connectivity preservation controller multi-agent systems by designing appropriate weights to a potential function to different agents [9]. The literature [11] presented a bounded input to implement a distributed connectivity maintenance controller for a first-order system with stationary leaders. Reference [12] studied the connectivity preservation problems for a multi-robot system with bounded control. A distributed connectivity preservation controller for Euler–Lagrange systems with time-delay and bounded actuation is designed in [13]. However, the connectivity preservation study for SFF has not been investigated. Literature [14] provided a potential function based control method to avoid the collisions between spacecraft and preserve the connectivity of communication networks simultaneously. The connectivity preservation problem of leader-follower Lagrange systems is studied, and simulations with spacecraft relative dynamics are proposed in [15]. However, the above studies did not consider the collision avoidance problem in formation.

The challenge now is to design distributed controllers for spacecraft in consideration of bounded actuation, connectivity preservation, and collision avoidance at the same time. Inspired by the previous discussions, this paper proposes a distributed controller with indirect couplings and bounded artificial potential functions. Firstly, the communication graph between spacecraft is defined according to the relative distances between all spacecraft. Then, a bounded artificial potential function is presented. Moreover, a local second-order virtual proxy spacecraft is designed for each spacecraft. The virtual proxy and the spacecraft are coupled with a saturated P+d controller. Finally, the virtual proxies are connected through the two potential functions. Numerical simulations confirm the effectiveness of the anti-saturation distributed connectivity preservation controller.

2 Background

2.1 Spacecraft Relative Dynamics

Consider a system with N rigid spacecraft denoted by $\boldsymbol{p}_i = [p_{ix}, p_{iy}, p_{iz}]^\top$ in the reference frame, the relative dynamics of the spacecraft are described by [16]

$$m_i \ddot{\boldsymbol{p}}_i = m_i \boldsymbol{C}_i \dot{\boldsymbol{p}}_i + m_i g_i(\boldsymbol{p}_i) + \boldsymbol{f}_i, \tag{1}$$

where

$$\boldsymbol{C}_i = 2\dot{\theta}_0 \begin{bmatrix} 0 & 1 & 0 \\ -1 & 0 & 0 \\ 0 & 0 & 0 \end{bmatrix},$$

$$g_i(\boldsymbol{p}_i) = \frac{\mu}{r_i^3}\boldsymbol{p}_i - \begin{bmatrix} \dot{\theta}_0^2 & \ddot{\theta}_0 & 0 \\ -\ddot{\theta}_0 & \dot{\theta}_0^2 & 0 \\ 0 & 0 & 0 \end{bmatrix} \boldsymbol{p}_i - \mu \begin{bmatrix} -\frac{r_0}{r_i^3} + \frac{1}{r_0^2} \\ 0 \\ 0 \end{bmatrix},$$

and m_i denotes the mass of the spacecraft i, $\boldsymbol{f}_i$ denotes the control input to be designed, μ is the gravitational constant of the Earth, θ_0 denotes the true anomaly of the reference spacecraft, r_0 denotes the distance of the origin of the reference frame to the Earth's center, $r_i = \sqrt{(r_0 + p_{ix})^2 + p_{iy}^2 + p_{iz}^2}$ represents the distance between the Earth's center and the centroid of the spacecraft i.

2.2 *Algebraic Graph Theory*

The distance-induced proximity graph can be modeled by graph theory. Some notions of graph theory are presented in this subsection [17]. A undirected graph is denoted as $\mathcal{G}(\mathcal{V}, \mathcal{E})$, where $\mathcal{V} = \{1, 2, \ldots, N\}$ denotes the vertex set and $\mathcal{E} \subset \mathcal{V} \times \mathcal{V}$ denotes the edge set. An edge $(i, j) \in \mathcal{E}$ if the vertex i can communicate with the vertex j, and they are called a neighbor of each other. The neighbor set of vertex i is defined as $\mathcal{N}_i = \{j \in \mathcal{V}(i, j) \in \mathcal{E}\}$. A path of $\mathcal{G}$ is defined as an edge sequence $(i_1, i_2), (i_2, i_3), \ldots$, where $(i_k, i_{k+1}) \in \mathcal{E}$ $(k = 1, 2, \ldots)$. A graph $\mathcal{G}$ is called connected if there is a path between any two vertices in $\mathcal{V}$. The adjacency matrix $\boldsymbol{A}(\mathcal{G}) = [a_{ij}] \in \mathbb{R}^{N\times N}$ and the Laplacian matrix $\boldsymbol{L}(\mathcal{G}) = [l_{ij}] \in \mathbb{R}^{N\times N}$ are defined as

$$a_{ij} = \begin{cases} 1, & \text{if } (i, j) \in E(\mathcal{G}); \\ 0, & \text{otherwise.} \end{cases}$$

$$l_{ij} = \begin{cases} \sum_{j=1}^{N} a_{ij}, & \text{if } i = j; \\ -a_{ij}, & \text{otherwise.} \end{cases}$$

Lemma 1 *The Laplacian matrix $\boldsymbol{L}(\mathcal{G})$ is positive semidefinite if the graph $\mathcal{G}$ is connected [17].*

2.3 The Dynamic Graph Model

It is assumed that the neighbor relationship among the spacecraft is based on their relative distance. Suppose all spacecraft have the same sensing distance Δ. The collision distance between spacecraft is denoted as δ. The adjacency matrix $\boldsymbol{A}(\mathcal{G})$ between all spacecraft is generated dynamically according to the current distances as follows:

$$a_{ij}(t) = \begin{cases} 1, & \text{if } ||\boldsymbol{p}_{ij}(t)|| \in (\bar{\delta}, \bar{\Delta}), i, j \in \mathcal{V}\}; \\ 0, & \text{otherwise}; \end{cases} \tag{2}$$

where $\bar{\delta} = \delta + \nu_1$ and $\bar{\Delta} = \Delta - \nu_2$, $\boldsymbol{p}_{ij}(t) = \boldsymbol{p}_i(t) - \boldsymbol{p}_j(t)$, $a_{ij} = 1$ indicates spacecraft i can get the states of spacecraft j.

Assumption 1 The initial graph $\mathcal{G}(0)$ generated according to Eq. (2) is a connected graph, and no collisions occurs at the initial time.

Definition 1 ([18]) The desired formation configuration $\boldsymbol{p}_d$ is reachable if the following conditions hold

$$d_{ij} < \Delta, \forall i \in \{1, \ldots, N\}, j \in \mathcal{N}_i,$$

where $d_{ij} = ||\boldsymbol{p}_i^d - \boldsymbol{p}_j^d||$ represents the desired distance between spacecraft i and j.

Assumption 2 The desired formation $\boldsymbol{p}_d$ is reachable.

Assumption 3 The saturation bound is enough to balance the virtual gravity item g_i in Eq. (1), i.e., $\bar{\boldsymbol{f}}_i$ satisfies $|g_i| \leq \bar{g}_i \leq \bar{\boldsymbol{f}}_i$, where $\bar{\boldsymbol{f}}_i$ is the saturation bound for each spacecraft.

Assumption 4 All spacecraft are initially at rest, i.e., $\dot{\boldsymbol{p}}_i(0) = 0$.

Remark 1 It is generally infeasible for bounded control input to preserve the connectivity of a second-order system and the same as Eq. (1). An example is shown in [19]. Therefore, the Assumption 4 is reasonable.

2.4 Artificial Potential Function

To design the distributed controller, a bounded artificial potential function $J\left(\|\hat{\boldsymbol{p}}_{ij}\|\right)$ is given as

$$J\left(\|\hat{\boldsymbol{p}}_{ij}\|\right) = \begin{cases} PJ^r\left(\|\hat{\boldsymbol{p}}_{ij}\|\right), & \text{if } ||\hat{\boldsymbol{p}}_{ij}|| \in \left[\hat{\delta}, d_{ij}\right]; \\ PJ^a\left(\|\hat{\boldsymbol{p}}_{ij}\|\right), & \text{if } ||\hat{\boldsymbol{p}}_{ij}|| \in \left[d_{ij}, \hat{\Delta}\right]; \end{cases} \tag{3}$$

where

$$J^r\left(\left\|\hat{\boldsymbol{p}}_{ij}\right\|\right)=\frac{\left(\left\|\hat{\boldsymbol{p}}_{ij}\right\|-d\right)^2\left(\hat{\Delta}-\left\|\hat{\boldsymbol{p}}_{ij}\right\|\right)}{\left\|\hat{\boldsymbol{p}}_{ij}\right\|-\hat{\delta}+\frac{(d-\hat{\delta})^2\left(\hat{\Delta}-\left\|\hat{\boldsymbol{p}}_{ij}\right\|\right)}{Q}}, \tag{4}$$

$$J^a\left(\left\|\hat{\boldsymbol{p}}_{ij}\right\|\right)=\frac{\left(\left\|\hat{\boldsymbol{p}}_{ij}\right\|-\hat{\delta}\right)\left(\left\|\hat{\boldsymbol{p}}_{ij}\right\|-d\right)^2}{\left(\hat{\Delta}-\left\|\hat{\boldsymbol{p}}_{ij}\right\|\right)+\frac{\left(\left\|\hat{\boldsymbol{p}}_{ij}\right\|-\hat{\delta}\right)(\hat{\Delta}-d)^2}{Q}}, \tag{5}$$

with $\hat{\Delta}=\Delta-\epsilon_1$, $\hat{\delta}=\delta+\epsilon_2$, P and Q are positive constant. It can be verified that $J(d)=0$ and $J(\hat{\delta})=J(\hat{\Delta})=PQ$.

Lemma 2 *The potential function J is monotonically increasing in regard to $||\hat{\boldsymbol{p}}_{ij}||$ while $||\hat{\boldsymbol{p}}_{ij}||\in(d,\hat{\Delta})$, and monotonically decreasing while $||\hat{\boldsymbol{p}}_{ij}||\in(\hat{\delta},d)$.*

Proof We prove the monotonicity of the repulsive potential function $J^r\left(\left\|\hat{\boldsymbol{p}}_{ij}\right\|\right)$. The proof of $J^a\left(\left\|\hat{\boldsymbol{p}}_{ij}\right\|\right)$ is omitted due to similarity. To simplify, the repulsive function is denoted as

$$J^r(x)=\frac{(x-d)^2\left(\hat{\Delta}-x\right)}{x-\hat{\delta}+\bar{Q}(\hat{\Delta}-x)},\ x\in\left(\hat{\delta},d\right) \tag{6}$$

where $x=\left\|\hat{\boldsymbol{p}}_{ij}\right\|$ and $\bar{Q}=\frac{(d-\hat{\delta})^2}{Q}$. The partial derivative of Eq. (6) can be written as

$$\begin{aligned}\frac{\partial J^r(x)}{\partial x}=&\frac{\left[2(\hat{\Delta}-x)(x-d)-(x-d)^2\right]\left[x-\hat{\delta}+\bar{Q}(\hat{\Delta}-x)\right]}{\left[x-\hat{\delta}+\bar{Q}(\hat{\Delta}-x)\right]^2}\\&+\frac{(\bar{Q}-1)(\hat{\Delta}-x)(x-d)^2}{\left[x-\hat{\delta}+\bar{Q}(\hat{\Delta}-x)\right]^2}\\=&\frac{(x-d)\left[2(\hat{\Delta}-x)-(x-d)\right](x-\hat{\delta})-(\hat{\Delta}-x)(x-d)^2}{\left[x-\hat{\delta}+\bar{Q}(\hat{\Delta}-x)\right]^2}\\&+\frac{2\bar{Q}(x-d)(\hat{\Delta}-x)^2}{\left[x-\hat{\delta}+\bar{Q}(\hat{\Delta}-x)\right]^2}\end{aligned} \tag{7}$$

Since the denominator is positive, it only needs to ensure the numerator is negative. The numerator can be written as

$$\begin{aligned}&(x-d)\left[2(\hat{\Delta}-x)-(x-d)\right](x-\hat{\delta})-(\hat{\Delta}-x)(x-d)^2+2\bar{Q}(x-d)(\hat{\Delta}-x)^2\\=&(x-d)\left[(2\hat{\Delta}+d-3x)(x-\hat{\delta})+(\hat{\Delta}-x)(d-x)+2\bar{Q}(\hat{\Delta}-x)^2\right]\end{aligned} \tag{8}$$

Note that $x \in [\hat{\delta}, d]$ and $\hat{\Delta} > d$, Eq. (8) is negative for all $x \in (\hat{\delta}, d)$. Therefore, Eq. (7) is negative and further implies that $J^r(\|\hat{\boldsymbol{p}}_{ij}\|)$ is monotonically decreasing in regard to x while $x \in (\hat{\delta}, d_{ij})$. ■

Remark 2 The potential function used in [20] is generated by adding the repulsive potential function and attractive potential function. However, the function might have several minima as J^r and J^a might affect the monotonicity of each other. We give a severe proof in Lemma 2 to ensure that the potential function has only one minimum.

3 Controller Design with Bounded Actuation

In this section, we present a distributed controller with bounded actuation constraints. Define the following virtual proxy system for each spacecraft

$$\ddot{\hat{\boldsymbol{p}}}_i = \mathrm{Sat}_i\left(\alpha_i \tilde{\boldsymbol{p}}_i\right) - \sum_{j=1}^{N} a_{ij} \nabla_i J\left(\|\hat{\boldsymbol{p}}_{ij}\|\right) - \beta_i \dot{\hat{\boldsymbol{p}}}_i, \tag{9}$$

where $\hat{\boldsymbol{p}}_i$ denotes the position of the i-th proxy, $\tilde{\boldsymbol{p}}_i = \boldsymbol{p}_i - \hat{\boldsymbol{p}}_i$, α_i and β_i are positive constant, $\mathrm{Sat}_i(\boldsymbol{x})$ is a function saturates $\boldsymbol{x}$ component-wise with the bound $\bar{\boldsymbol{f}}_i^k - \bar{g}_i^k$, $k = 1, 2, 3$. The initial state of the virtual proxy is designed as

$$\hat{\boldsymbol{p}}_i(0) = \boldsymbol{p}_i(0),\ \dot{\hat{\boldsymbol{p}}}_i(0) = 0, i = 1, \ldots, N. \tag{10}$$

Lemma 3 *The virtual energy stored between spacecraft i and its virtual proxy is*

$$\psi_i\left(\tilde{\boldsymbol{p}}_i\right) = \int_0^{\tilde{\boldsymbol{p}}_i} \mathrm{Sat}_i\left(\alpha_i \boldsymbol{\sigma}\right)^\top d\boldsymbol{\sigma}. \tag{11}$$

The function has the following properties:

(1) $\psi_i\left(\tilde{\boldsymbol{p}}_i\right)$ *is a convex function.*
(2) Within the domain $B(\mathbf{0}, (\epsilon/2)) = \{\tilde{\boldsymbol{p}}_i | \, ||\tilde{\boldsymbol{p}}_i|| \leq (\epsilon/2)\}$, $\psi_i\left(\tilde{\boldsymbol{p}}_i\right)$ *achieves its maximum while* $\|\tilde{\boldsymbol{p}}_i\| = (\epsilon/2)$ *and its minimum while* $\|\tilde{\boldsymbol{p}}_i\| = (\epsilon/2)$.
(3) Let

$$\psi_i^{\min} = \min_{\tilde{\boldsymbol{p}}_i} \psi_i\left(\tilde{\boldsymbol{p}}_i\right) = \int_0^{\tilde{\boldsymbol{p}}_i} \mathrm{Sat}_i\left(\alpha_i \boldsymbol{\sigma}\right)^\top d\boldsymbol{\sigma},\ s.t.\ \|\tilde{\boldsymbol{p}}_i\| = \frac{\epsilon}{2}, \tag{12}$$

where $\epsilon = \min\{\epsilon_1, \epsilon_2\}$. *If* $\psi_i\left(\tilde{\boldsymbol{p}}_i\right) \leq \psi_i^{\min}$, *then* $\tilde{\boldsymbol{p}}_i \in B(\mathbf{0}, (\epsilon/2))$.

The proof of Lemma 3 is like the Propositions 1–3 in [13], and is omitted here.

Remark 3 By the triangle inequality $\|\boldsymbol{p}_{ij}\| \leq \|\tilde{\boldsymbol{p}}_i\| + \|\hat{\boldsymbol{p}}_{ij}\| + \|\tilde{\boldsymbol{p}}_j\|$, it is enough to ensure $\|\boldsymbol{p}_{ij}\| \leq [\delta, \Delta]$, $(i, j) \in \mathcal{E}$ while the following inequalities are satisfied:

$$\|\hat{\boldsymbol{p}}_{ij}\| \in \left[\hat{\delta}, \hat{\Delta}\right], \quad \|\tilde{\boldsymbol{p}}_i\| \leq \epsilon/2. \tag{13}$$

Remark 4 The energy function ψ_i could be regarded as a virtual artificial potential function between the spacecraft i and its proxy. While the input of the controller reaches saturation, the energy function gradually increases. While the input is not saturated and the energy function is greater than zero, the energy function will gradually decreases and eventually tends to zero.

Design the control input

$$\boldsymbol{f}_i = -\operatorname{Sat}_i(\alpha_i \tilde{\boldsymbol{p}}_i) - m_i g_i. \tag{14}$$

Consider the following Lyapunov candidate

$$V = V_k + V_p \tag{15}$$

where

$$V_k = \frac{1}{2}\sum_{i=1}^{N}\left(\dot{\boldsymbol{p}}_i^\top m_i \dot{\boldsymbol{p}}_i + \dot{\hat{\boldsymbol{p}}}_i^\top \dot{\hat{\boldsymbol{p}}}_i\right) \tag{16}$$

$$V_p = \frac{1}{2}\sum_{i=1}^{N}\sum_{j=1}^{N} a_{ij} J\left(\|\hat{\boldsymbol{p}}_{ij}\|\right) + \sum_{i=1}^{N}\psi_i\left(\tilde{\boldsymbol{p}}_i\right) \tag{17}$$

Lemma 4 *Given a system with dynamics Eq. (1) satisfies Assumptions 1–4, let* $M = |\mathcal{E}(0)|$, $\psi^{\min} = \min_{i=1,\ldots,N}\{\psi_i^{\min}\}$, *and select* Q *and* P *satisfy*

$$Q \geq \frac{\left[\left(\bar{\Delta} - d\right)^2 - (\hat{\Delta} - d)^2\right](\bar{\Delta} - \hat{\delta})}{\left(\hat{\Delta} - \bar{\Delta}\right)}, \tag{18}$$

$$P = \frac{\psi^{\min}}{Q}. \tag{19}$$

Then, $V(t) \leq V(0)$ *ensures* $\|\tilde{\boldsymbol{p}}_i(t)\| \leq (\epsilon/2)$ *and* $\|\boldsymbol{p}_{ij}\| \in [\delta, \Delta]$, $(i, j) \in \mathcal{E}$.

Proof By the initial configuration given in Eq. (10) and Assumption 4 and, we have $V_k(0) = 0$ and $\psi_i\left(\tilde{\boldsymbol{p}}_i(0)\right) = 0$, for $i = 1, \ldots, N$. Therefore,

$$
\begin{aligned}
V(0) =& \frac{1}{2}\sum_{i=1}^{N}\sum_{j=1}^{N} a_{ij} J\left(\|\hat{\boldsymbol{p}}_{ij}\|\right) < M\left[J(\bar{\Delta}) + J(\bar{\delta})\right] \\
\leq & J(\hat{\Delta}) = J(\hat{\delta}) = PQ = \psi^{\min}.
\end{aligned} \tag{20}
$$

If $V(t) \leq V(0)$ satisfies, it is obtained

$$
V_p(t) \leq V(t) \leq V(0) < J(\hat{\Delta}) = J(\hat{\delta}) = PQ = \psi^{\min}. \tag{21}
$$

Suppose the maximum distance among all initial connected edges is $||\hat{\boldsymbol{p}}_{lm}(t)|| = \hat{\Delta}$. This implies $V_p(t) \geq J(||\hat{\boldsymbol{p}}_{lm}(t)||) = PQ$, which contradicts Eq. (21). Therefore, all distances $||\hat{\boldsymbol{p}}_{ij}(t)|| < \hat{\Delta}$, $(i, j) \in \mathcal{E}$. Using a similar procedure, it is obtained $||\hat{\boldsymbol{p}}_{ij}(t)|| > \hat{\delta}$.

Since $J(||\hat{\boldsymbol{p}}_{ij}||) \geq 0$, Eqs. (17) and (21) implies $\psi_i\left(\tilde{\boldsymbol{p}}_i\right) \leq \psi^{\min}$. According to the property (3) of Eq. (11), it is obtained that $\left\|\tilde{\boldsymbol{p}}_i(t)\right\| \leq (\epsilon/2)$. Therefore, we have

$$
\begin{aligned}
\left\|\boldsymbol{p}_{ij}\right\| \leq \left\|\hat{\boldsymbol{p}}_{ij}\right\| + \left\|\tilde{\boldsymbol{p}}_i\right\| + \left\|\tilde{\boldsymbol{p}}_j\right\| < \hat{\Delta} + 2\cdot(\epsilon/2) < \Delta, \\
\left\|\boldsymbol{p}_{ij}\right\| \geq \left\|\hat{\boldsymbol{p}}_{ij}\right\| - \left\|\tilde{\boldsymbol{p}}_i\right\| - \left\|\tilde{\boldsymbol{p}}_j\right\| > \hat{\delta} - 2\cdot(\epsilon/2) > \delta.
\end{aligned} \tag{22}
$$

In conclusion, $\left\|\boldsymbol{p}_{ij}\right\| \in [\delta, \Delta]$, $(i, j) \in \mathcal{E}$, i.e., there are no collisions between spacecraft and all communication links between all adjacent spacecraft are preserved. ■

Theorem 1 *Given a system with dynamics Eq.* (1) *satisfies Assumptions 1–4 and Q and P are given in Eqs. (18) and* (19)*. Then the control inputs in Eqs. (9) and (14) can achieve the desired formation, the collision avoidances and the connectivity preservation.*

Proof Taking the derivative of Eq. (16) and substituting Eqs. (1), (9) and (14) into it yields

$$
\begin{aligned}
\dot{V}_k(t) =& \sum_{i=1}^{N} \dot{\boldsymbol{p}}_i^{\top}\left[m_i \boldsymbol{C}_i \dot{\boldsymbol{p}}_i + m_i g_i - \mathrm{Sat}_i(\alpha_i \tilde{\boldsymbol{p}}_i) - m_i g_i\right] \\
&+ \sum_{i=1}^{N} \dot{\hat{\boldsymbol{p}}}_i^{\top}\left[\mathrm{Sat}_i\left(\alpha_i \tilde{\boldsymbol{p}}_i\right) - \sum_{j=1}^{N} a_{ij}\nabla_i J\left(\|\hat{\boldsymbol{p}}_{ij}\|\right) - \beta_i \dot{\hat{\boldsymbol{p}}}_i\right] \\
=& -\sum_{i=1}^{N} \dot{\tilde{\boldsymbol{p}}}_i^{\top} \mathrm{Sat}_i(\alpha_i \tilde{\boldsymbol{p}}_i) - \sum_{i=1}^{N} \dot{\hat{\boldsymbol{p}}}_i^{\top} \sum_{j=1}^{N} a_{ij}\nabla_i J\left(\|\hat{\boldsymbol{p}}_{ij}\|\right) - \beta_i \sum_{i=1}^{N} \dot{\hat{\boldsymbol{p}}}_i^{\top} \dot{\hat{\boldsymbol{p}}}_i.
\end{aligned} \tag{23}
$$

According to the definition of V_p in Eq. (17), the derivative of it can be written as

$$
\begin{aligned}
\dot{V}_p(t) =& \frac{1}{2}\sum_{i=1}^{N}\sum_{j=1}^{N} a_{ij}\left[\nabla_i J\left(\left\|\hat{\boldsymbol{p}}_{ij}\right\|\right)\dot{\hat{\boldsymbol{p}}}_i + \nabla_j J\left(\left\|\hat{\boldsymbol{p}}_{ij}\right\|\right)\dot{\hat{\boldsymbol{p}}}_j\right] + \sum_{i=1}^{N}\dot{\hat{\boldsymbol{p}}}_i^{\top}\,\mathrm{Sat}_i(\alpha_i\tilde{\boldsymbol{p}}_i) \\
=& \sum_{i=1}^{N}\sum_{j=1}^{N} a_{ij}\nabla_i J\left(\left\|\hat{\boldsymbol{p}}_{ij}\right\|\right)\dot{\hat{\boldsymbol{p}}}_i + \sum_{i=1}^{N}\dot{\hat{\boldsymbol{p}}}_i^{\top}\,\mathrm{Sat}_i(\alpha_i\tilde{\boldsymbol{p}}_i).
\end{aligned} \tag{24}
$$

By summing Eqs. (23) and (24), the derivative of V yields

$$
\begin{aligned}
\dot{V}(t) =& -\sum_{i=1}^{N}\dot{\hat{\boldsymbol{p}}}_i^{\top}\,\mathrm{Sat}_i(\alpha_i\tilde{\boldsymbol{p}}_i) - \sum_{i=1}^{N}\dot{\hat{\boldsymbol{p}}}_i^{\top}\sum_{j=1}^{N} a_{ij}\nabla_i J\left(\|\hat{\boldsymbol{p}}_{ij}\|\right) - \beta_i\sum_{i=1}^{N}\dot{\hat{\boldsymbol{p}}}_i^{\top}\dot{\hat{\boldsymbol{p}}}_i \\
&+ \sum_{i=1}^{N}\sum_{j=1}^{N} a_{ij}\nabla_i J\left(\left\|\hat{\boldsymbol{p}}_{ij}\right\|\right)\dot{\hat{\boldsymbol{p}}}_i + \sum_{i=1}^{N}\dot{\hat{\boldsymbol{p}}}_i^{\top}\,\mathrm{Sat}_i(\alpha_i\tilde{\boldsymbol{p}}_i) \\
=& -\beta_i\sum_{i=1}^{N}\dot{\hat{\boldsymbol{p}}}_i^{\top}\dot{\hat{\boldsymbol{p}}}_i.
\end{aligned} \tag{25}
$$

Therefore, $\dot{V}(t) \le 0$ and $V(t) \le V(0)$. Lemma 4 further indicates that $\left\|\boldsymbol{p}_{ij}\right\| \in$ $(i, j) \in \mathcal{E}$, i.e., the connectivity preservation and the collisions avoidance are achieved. Equation (25) also ensures that $\dot{\boldsymbol{p}}_i$, $J(\hat{\boldsymbol{p}}_i)$, $\psi(\tilde{\boldsymbol{p}}_i) \in \mathcal{L}_\infty$ and $\dot{\hat{\boldsymbol{p}}}_i \in \mathcal{L}_2 \cap \mathcal{L}_\infty$. Therefore, $\dot{\hat{\boldsymbol{p}}}_i \to \mathbf{0}$ as $t \to \infty$. Since $J(\hat{\boldsymbol{p}}_i)$ is continuously differentiable and bounded, we have $\nabla_i J(\hat{\boldsymbol{p}}_i) \in \mathcal{L}_\infty$. Taking the derivative of Eq. (9) implies that $\dddot{\hat{\boldsymbol{p}}}_i \in \mathcal{L}_\infty$ and $\ddot{\hat{\boldsymbol{p}}}_i \to \mathbf{0}$. The secondary derivative of Eq. (9) further implies $\dddot{\hat{\boldsymbol{p}}}_i \to \mathbf{0}$. Therefore, $\ddot{\tilde{\boldsymbol{p}}}_i \to \mathbf{0}$, $\nabla_i J(||\hat{\boldsymbol{p}}_i||) \to \mathbf{0}$, $(i, j) \in \mathcal{E}$ and $||\hat{\boldsymbol{p}}_i|| \to d_{ij}$. By noting $\ddot{\hat{\boldsymbol{p}}}_i \to \mathbf{0}$ and $\dot{\hat{\boldsymbol{p}}}_i \to \mathbf{0}$, Eq. (9) leads to $\tilde{\boldsymbol{p}}_i \to \mathbf{0}$. Overall, $||\boldsymbol{p}_i|| \to d_{ij}$, $(i, j) \in \mathcal{E}$, i.e., the desired formation is achieved. ■

Remark 5 The parameters in Eq. (14) can be designed as follows:

(1) Compute $\psi_i^{\min}$ according to (12);
(2) Select Q satisfy Eq. (18);
(3) Compute P according to (19).

4 Simulations

To confirm the effectiveness of the bounded actuation controller in (14) and (9), a simulation with three spacecraft are presented in this section. The parameters of the reference orbit are given Table 1. The sensing radius of each spacecraft is set as $\Delta = 40$ m, and the anti-collision distance is given as $\delta = 10$ m. The masses of all spacecraft are $m_i = 10$ kg, $i = 1, 2, 3$.

The initial positions of three spacecraft are $\boldsymbol{p}_1(0) = [-40, -30, 0]^{\top}$ m, $\boldsymbol{p}_2(0) = [-15, -40, 5]^{\top}$ m, $\boldsymbol{p}_3(0) = [0, -40, 0]^{\top}$ m, the velocities are $\boldsymbol{v}_i(0) = [0, 0, 0]^{\top}$ (m/s),

Table 1 Parameters for the reference orbit

Orbital parameters	Value
Eccentricity	0.01
Inclination	0°
Longitude ascending node	20°
Semi-major axis	6971 km
Argument of perigee	30°
Initial true anomaly	20°
Gravitational parameter	3.986×10^{14} (m^3/s^2)

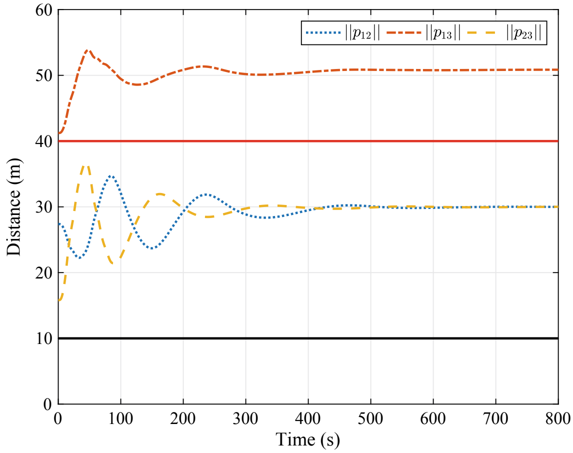

Fig. 1 The distances between spacecraft

$i = 1, 2, 3$. The desired distance between all spacecraft are $d_{12} = 30\,\text{m}$, $d_{13} = 50\,\text{m}$, $d_{23} = 30\,\text{m}$. It is easy to verify that the Assumptions 1 and 2 are satisfied. The parameters are given as $Q = 10000$, $P = 0.002$, $\alpha_i = 0.2$, $\beta_i = 0.1$, $\bar{f}_i = 0.5$ N, $\bar{f}_i - \bar{g}_i = 0.4$ N.

Figure 1 presents the distance between three spacecraft over time, where the red line represents the communication distance of the spacecraft, and the black line represents the anti-collision distance between the spacecraft. The figure indicates that the distances $||\boldsymbol{p}_{12}||$ and $||\boldsymbol{p}_{23}||$ has never exceeded the communication range. The connectivity of the the graph is preserved. Figure 2 demonstrates the velocity of all three spacecraft eventually converged to zero. Figure 3 presents that the distance errors between the spacecraft and its virtual proxy spacecraft are not more than 4 m, and it finally converges to zero. Figure 4 shows that the velocity errors between the spacecraft and the virtual proxy also eventually converged to zero. Figure 5 gives the time-varying control inputs applied to each spacecraft. It can be seen from the figure that the maximum amplitude of the control inputs is less than 0.5 N, which satisfies the saturation condition.

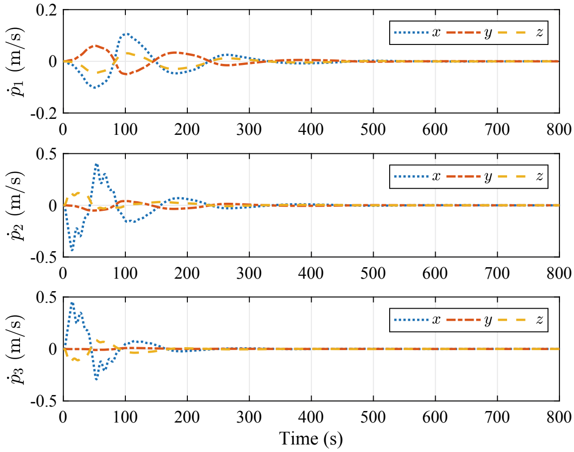

Fig. 2 The velocities of spacecraft

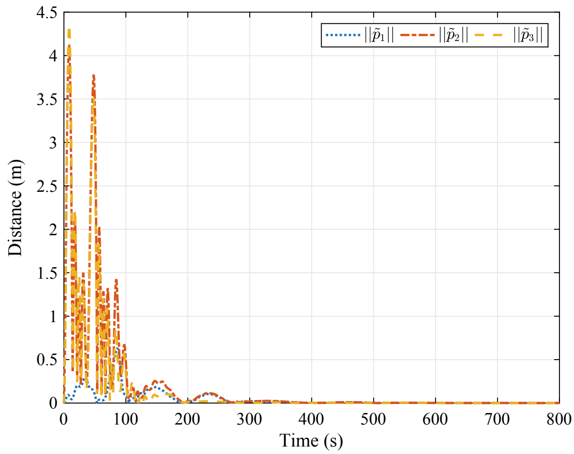

Fig. 3 The distances between spacecraft and proxies

5 Conclusions

This paper considered the impact of actuator saturation on connectivity preservation and collision avoidance control of SFF. An indirect coupling strategy with bounded artificial potential function is proposed to overcome actuator saturation constraints. The proposed control algorithm is also applicable to other Lagrangian systems. In future work, the connectivity preservation of directed graph in the presence of actuator saturation will be studied.

Fig. 4 The velocity errors between spacecraft and proxies

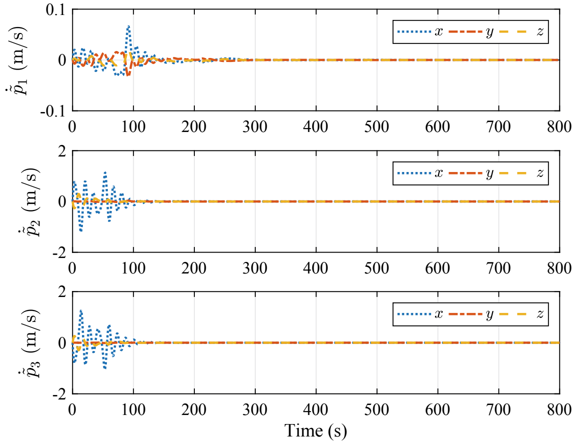

Fig. 5 The control inputs

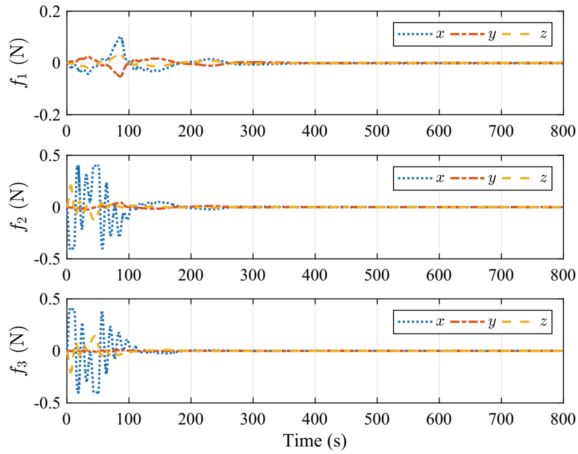

References

1. Liu, G., Zhang, S.: A survey on formation control of small satellites. Proc. IEEE **106**(3), 440–457 (2018)
2. Zou, A.M., de Ruiter, A.H., Kumar, K.D.: Distributed finite-time velocity-free attitude coordination control for spacecraft formations. Automatica **67**, 46–53 (2016)
3. Yue, X., Xue, X., Wen, H., Yuan, J.: Adaptive control for attitude coordination of leader-following rigid spacecraft systems with inertia parameter uncertainties. Chin. J. Aeronaut. **32**(2), 688–700 (2019)
4. Knorn, S., Chen, Z., Middleton, R.H.: Overview: collective control of multiagent systems. IEEE Trans. Control Netw. Syst. **3**(4), 334–347 (2016)
5. Zavlanos, M.M., Pappas, G.J.: Potential fields for maintaining connectivity of mobile networks. IEEE Trans. Robot. **23**(4), 812–816 (2007)
6. Stephan, J., Fink, J., Kumar, V., Ribeiro, A.: Concurrent control of mobility and communication in multirobot systems. IEEE Trans. Robot. **33**(5), 1248–1254 (2017)

7. Kim, Y., Mesbahi, M.: On maximizing the second smallest eigenvalue of a state-dependent graph Laplacian. IEEE Trans. Autom. Control **51**(1), 116–120 (2006)
8. Qu, Z., Li, C., Lewis, F.: Cooperative control with distributed gain adaptation and connectivity estimation for directed networks. Int. J. Robust Nonlinear Control **24**(3), 450–476 (2014)
9. Ji, M., Egerstedt, M.: Distributed coordination control of multiagent systems while preserving connectedness. IEEE Trans. Robot. **23**(4), 693–703 (2007)
10. Cao, Y., Ren, W.: Distributed coordinated tracking with reduced interaction via a variable structure approach. IEEE Trans. Autom. Control **57**(1), 33–48 (2012)
11. Ajorlou, A., Momeni, A., Aghdam, A.G.: A class of bounded distributed control strategies for connectivity preservation in multi-agent systems. IEEE Trans. Autom. Control **55**(12), 2828–2833 (2010)
12. Gasparri, A., Sabattini, L., Ulivi, G.: Bounded control law for global connectivity maintenance in cooperative multirobot systems. IEEE Trans. Robot. **33**(3), 700–717 (2017)
13. Yang, Y., Shi, Y., Constantinescu, D.: Connectivity-preserving synchronization of time-delay Euler-Lagrange networks with bounded actuation. IEEE Trans. Cybern. (2019)
14. Xue, X., Yue, X., Yuan, J.: Distributed connectivity maintenance and collision avoidance control of spacecraft formation flying. In: 2019 Chinese Control Conference (CCC), pp. 8265–8270. IEEE (2019)
15. Ghapani, S., Mei, J., Ren, W., Song, Y.: Fully distributed flocking with a moving leader for Lagrange networks with parametric uncertainties. Automatica **67**, 67–76 (2016)
16. Kristiansen, R., Nicklasson, P.J.: Spacecraft formation flying: a review and new results on state feedback control. Acta Astronautica **65**(11–12), 1537–1552 (2009)
17. Mesbahi, M., Egerstedt, M.: Graph Theoretic Methods in Multiagent Networks, vol. 33. Princeton University Press, Princeton (2010)
18. Li, X., Sun, D., Yang, J.: A bounded controller for multirobot navigation while maintaining network connectivity in the presence of obstacles. Automatica **49**(1), 285–292 (2013)
19. Yang, Y., Constantinescu, D., Shi, Y.: Connectivity-preserving consensus of multi-agent systems with bounded actuation (2018). arXiv:1803.09309
20. Wen, G., Duan, Z., Su, H., Chen, G., Yu, W.: A connectivity-preserving flocking algorithm for multi-agent dynamical systems with bounded potential function. IET Control Theory Appl. **6**(6), 813–821 (2012)